Int. J. Electrochem. Sci., 12 **(2017)** 2242 – 2252, doi: 10.20964/2017.03.74

International Journal of
ELECTROCHEMICAL
SCIENCE
www.electrochemsci.org

Electrochemical Determination of Maltol in Food Sample Based on Nitrogen-Doped Graphene -Modified Electrode

Huacheng Tang[*], *Zhijiang Li, Ying Wang and Changyuan Wang*

College of Food science, Heilongjiang Bayi Agricultural University, Daqing 163319, Heilongjiang, P,R, China
[*]E-mail: huachengtang_163@qq.com

Received: 23 December 2016 / *Accepted:* 19 January 2017 / *Published:* 12 February 2017

There is an easily accessible and low cost approach to generating nitrogen-doped graphene (NG). This method is shown through the combination of high exfoliation speed and covalent metamorphose from the melamine (MA)–graphene oxide (GO) mixture. NGs processed during the temperature of 300, 600, and 900 °C featured X-ray photoelectron spectroscopy (XPS) in a systematic way. As for XPS, graphitic-N, pyridinic-N, as well as pyrrolic-N and are regarded to be three major nitrogen-doped frameworks with different proportions. NG modified GCE exerted a strengthening influence on the electrochemical oxidation process. After optimization, the anodic ultimate current of maltol react was in accordance with its concentration ranging from 0.05 μM to 70 μM, along with the detection limit of 0.02 μM, has been obtained.

Keywords: Graphene; Maltol; N-Doping; Electrochemical oxidation; Annealing temperature

1. INTRODUCTION

In spite of being a natural compound, maltol (3-hydroxy-2-methyl-4-Hpyran-4-one) could also been generated through thermally degrading sucrose as well as starch [1]. What food tastes could be transform or strengthen by maltol added in them, thought it is nearly without taste in case of under levelled concentration. Therefore, in food products like breads, beers, cakes, chocolate milk, malt beverages, maltol gains widespread application. On the other hand, this natural compound shows a toxicity working on the basis of certain dose, with the intermediary mechanism of apoptosis [2]. In addition, maltol could tremendously enhance gallium's oral bioavailability of as well as the absorption of aluminium because it is in harmony with such materials [3, 4]. The Legislation of EU regulates that 200 mg/kg is the ultimate restriction line for maltol in food products [5]. Thus, in the field of food

products, it is of vital significance to work out cost-effective as well as convenient approaches to maltol determination.

As for the issue of maltol determination, researchers has worked out diverse approaches like spectrophotometry [6-8], gas chromatographymass spectrometry (GC–MS) [9], liquid chromatography amperometric probing (LC–ED) [10], efficient liquid chromatography (HPLC) [11, 12], and FIA chemiluminescence [13]. Meanwhile, such approaches have diverse disadvantages like high inertness. Besides, such methods require equipment of high cost and huge amounts of organic solvents. In addition, they include process that cost plenty of time, which make regular analysis tremendously hard. Recently, being efficient, convenient, highly sensitive, reproducible as well as selectable, electrochemical sensors have gained widespread focus. Diverse electrodes based on modifier have been issued for elevating the sensitivity of detecting diverse mole cules [14-17]. Up to now, there have been a few voltammetric approaches to maltol determination issued with the adoption of diverse electrodes like carbon paste electrode [5], hanging mercury drop electrode [18], multiwalled carbon nanotubes modified electrode [19], silica sol–gel modified electrode [20].

As a substance in the form of carbon existing in with double dimensions, Graphene has gained tremendous focus when it comes to nanoelectronics, energy storage, and biosensors recently [20-22] because of its particular physicochemical traits of grapheme like high surface location, advanced performance in conducting ability, convenient generation as well as abundant appearance chemistry. In this way, graphene was suggested to be a potential medium in the field of energy storage/conversion devices, electric equipments, bioelectronics, as well as biosensors. However, graphene's traits concerning physic-chemistry as well as functionality rely on resultant grapheme's tiny structures as for edge effects, functional groups, as well as size to a large extent. Thus, lots of studies strive to produce favorable functional capacity of graphene through control of microstructure.

Researchers in this field put forward many approaches to modifying or strengthening the physico-chemical traits of grapheme like chemical functioning mechanism [23], graphene hybrids [24], as well as internal chemical mixture with heteroatoms . In such approaches, chemical doping is regarded to be an effective method of increasing the concentration of deliverer for charge shift as well as to elevate the capacity of conduction in an electrical way [25]. Nitrogen is regarded to be a promising constituent to achieve chemical doping in at it has nearly the same atom size and five valence electrons which could generate valence bonds in the existence of carbon atoms. Thus, graphene (NG) doped with nitrogen was put forward as material of use as for biosensors [26], and oxygen decrease [27], and electrical double-layer capacitors [28].

Under the circumstance of pyridinic-N, pyrrolic-N and graphitic-N types graphene modified electrode, this paper illustrates the voltammetric determination of maltol. In general, within the range of what we know, a detection and determination of maltol at this perspective type of electrochemical sensor has not gone through investigation in previous studies. The real applicability of the approach put forward is demonstrated in determining maltol in samples like beer and orange juice.

2. EXPERIMENTAL

2.1. Nitrogen-doped graphene (NG) preparation

The revised Hummer approach was used for preparing GO from raw graphite powders. GO weighing 25 mg was put into a 50-mL aqueous solution with 1 mM melamine (MA) in. Through the process of ultrasonication, the solution went through stir at ambient temperature for 8 h, followed by the drying of MA–GO, the resultant mixture at the temperature of 40 °C in the condition of vacuum. Prior to the process of expansion–exfoliation through thermal treatment, powders of MA–GO were allocated one-lateral of the quartz tube in a furnace with high temperature. Subsequently, through thermal treatment the central area of the above mentioned quartz tube increased to 300, 600, and 900 °C under the condition of vacuum. Then, the samples of MA–GO located on the lateral part were soon allocated towards the central area of the tuber and remained at the temperatures mentioned above for 2 h. When the furnace got cool, the resultant NGs, classified to be NG300, NG600 and NG900 remained within the container. GO was declined through thermal treatment with a nearly same process, under the specific temperature of 900 °C, to make preparation for the graphene sample.

2.2. Characterization

A PHI Quantera SXM conducted the analysis of X-ray photoelectron spectroscopy (XPS) with the use of an Al Kα X-ray source. The N_2adsorption/desorption isotherms went through measurement at 77 K (Autosorb-1, Quantachrome) in order for gaining information on certain surface spot and framework of pore. The experiments concerning electrochemistry went through measurement by putting a CHI 627D electrochemical analysis equipment in a cell with triple-electrode. One bare GCE or NG-modified GCE was adopted to be functioning electrode. One platinum-made wire and an Ag/AgCl electrode (3 M KCl) were respectively applied to be counter electrode and the reference.

2.3. Electrode modification

Before being modified, GCE went through polishment with alumina powder of 1.0 and 0.05 μm on cloth and sonication in succession in water-ethanol mixture (1:1, V/V) and water to withdraw particles that have been adsorbed. The NG/GCE was achieved by putting 10 μL of NG suspension on the GCE surface and dried with an infrared lamp.

2.4. Determination of maltol

Maltol determination was conducted through adopting boric acid-borax buffer with pH 8.2 as electrolyte. After being under open circuit for 60 s and being still for 5 s, the SWV was performed at rang of 0.10 to 0.90 V, with the oxidation ultimate current of 0.55 V for maltol. The frequency was15 Hz, the scan rate 40 mV/s, and the amplitude 25 mV. Cyclic voltammograms was performed in

pH 8.2 boric acid−borax buffer in presence of 10 μM maltol with a scan rate of 100 mV/s. DPV was performed in pH 8.2 boric acid−borax buffer from 0.3 to 0.8 V.

3. RESULT AND DISCUSSION

Table 1. Carbon, nitrogen and oxygen atomic percentages from GO, graphene and NGs prepared with diverse ultrafast thermal expansion-exfoliation temperatures.

	C (%)	N (%)	O (%)	C/O ratio	C/N ratio
GO	53.44	—	44.57	1.35	—
NG300	64.51	8.73	26.23	2.29	7.40
NG600	76.84	4.48	17.29	4.63	16.22
NG900	81.28	2.61	13.67	5.41	34.5

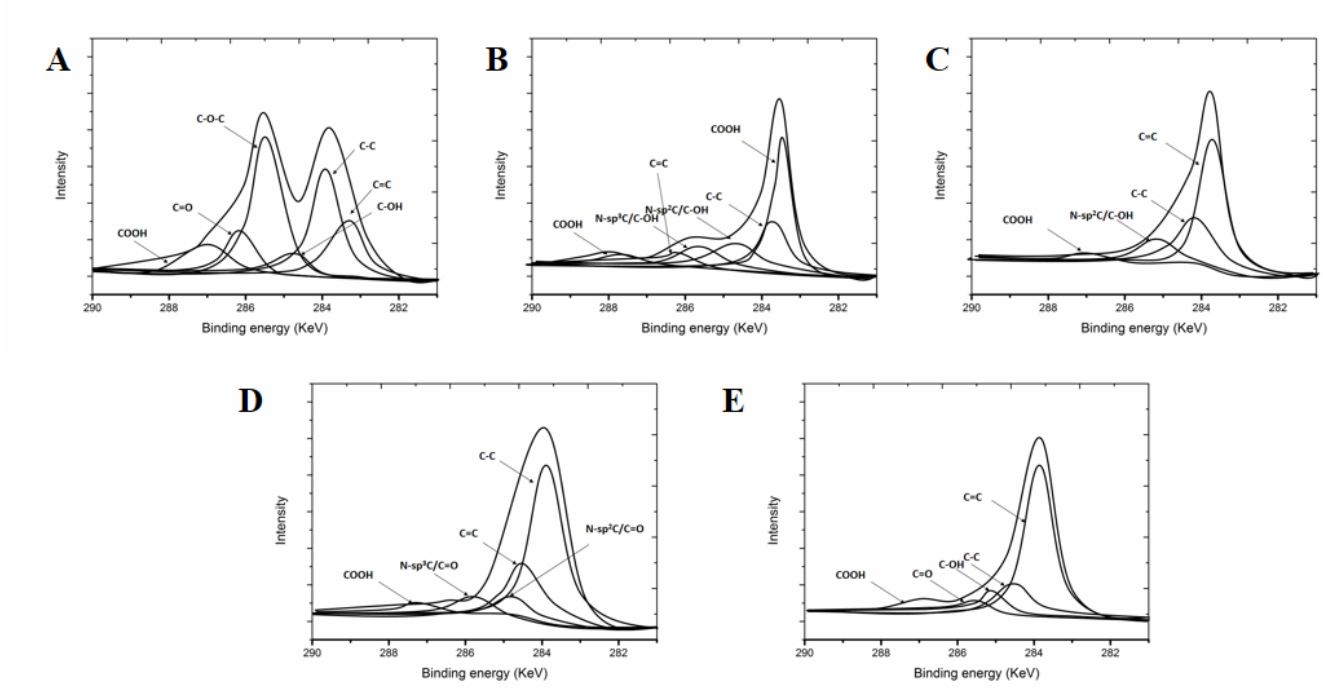

Figure 1. XPS C1s core level spectra of (A) GO, (B) NG300, (C) NG600, (D) NG900 and (E) graphene of the XPS spectra of the above materials.

In order to confirm nitrogen succeeded in doping into the graphene sheet frameworks at diverse temperatures of thermal expansion with extremely high speed, XPS was employed for analyzing nitrogen atoms appearance construction and chemical configuration in three NGs. Fig. 1A–E indicate the C1s core level spectra of GO, NG300, NG600, NG900 and graphene. Note that the C1s ultimate point of the materials mentioned above go through major classification into six peaks, corresponding to C=C (283.9 eV), C–C (284.2–285.1 eV), C_{sp2}–NH_2/C–OH (285.2 eV), C–O–C (286.2 eV), Csp^3–NH/C=O (287.4 eV) and O–C=O (288.1 eV). It demonstrated successful doping of N into the graphitic layer of graphene. The intensity peaks characteristic of the C−O groups increased, but those

characteristics of C−C decreased, indicating that doping not only introduced nitrogen atoms into host graphene but also increased the content of oxygen [29, 30]. In addition, note that two ultimate points of the C–N bonding share some similarities with those of C=O and C–OH. Compared to the XPS survey scan of GO, the proportion of atoms in oxygen on NG300, NG600, NG900 and graphene reduces to a large extent.

The atomic percentage of carbon and nitrogen of each material is indicated in Table 1. The ratio of C to O atoms on GO is 1.2, showing GO owns plenty of functional groups with oxygen in on its appearance. On the other hand, all the C/O ratios of NG300, NG600, NG900 and graphene rise to more elevated figures, which shows GO could decreased in an effective way after being thermally expanded with extremely high speed. Obviously, the C/O ratio rises from 2.2, 4.1 to 5.3, together with the temperature of above mentioned process rising from 300, 600 to 900 °C. Such outcome indicates that a more elevated ultrafast thermal expansion temperature leads to a more optimized decrease of GO. In addition, the C/O ratio of graphene is 5.7, a little bit more elevated than that of NG900, indicating that N atoms take the place of a few C atoms in graphene, leading to the reduction in the ratio of C/O. "However, the C/N ratio of N-doped graphenes rises too, as ultrafast thermal expansion temperature increases, which is indicated in Table 1. Such outcome shows that more elevated ultrafast thermal expansion temperature brings about GO decrease in a larger scale. The possible reason for little reduction of nitrogen at raised temperature might be more elevated degree of melamine's decomposition through thermal treatment".

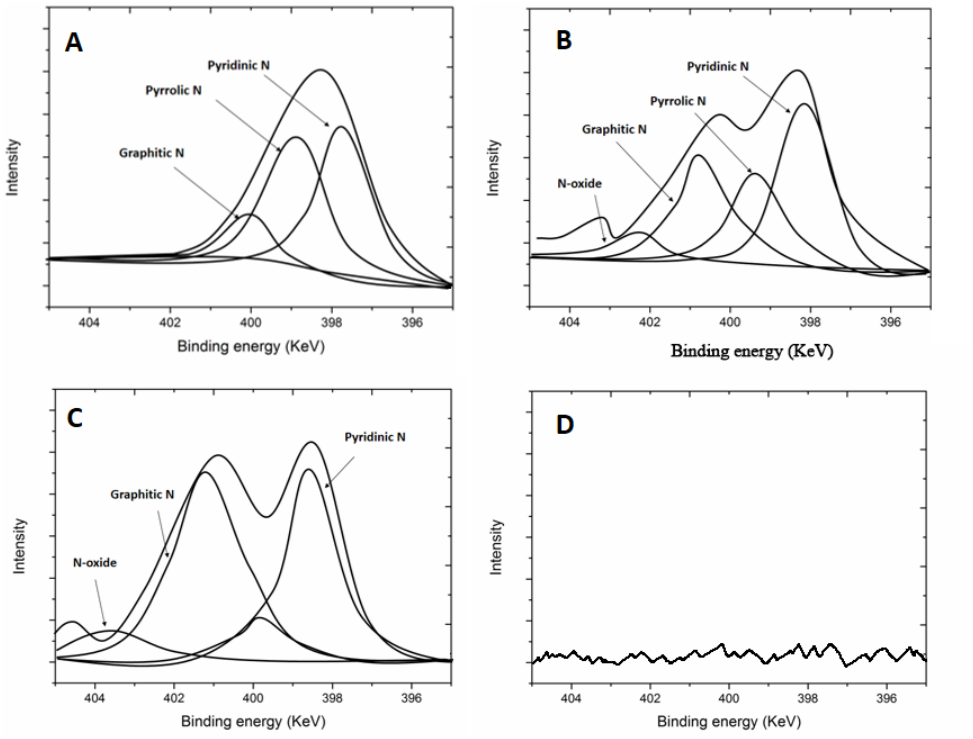

Figure 2. XPS N1s scans of (A) NG300, (B) NG600, (C) NG900 and (D) graphene.

Besides XPS C1s spectra, researchers also show N1s spectra for to further confirmation of how the nitrogen atoms are chemically configured and composed in three NGs mentioned above. In Fig. 2A–C, the occurrence of N1s ultimate point on every spectrum indicates that the nitrogen succeeds in doping into the graphene sheet in spite of the diverse expansion temperatures through thermal treatment at extremely high speed. All these N1s ultimate point spectra could go through separation into four elements: pyridinic-N, pyrrolic-N, graphitic-N and pyridine-N-oxide [31-34]. On the other hand, the ratio of such groups with nitrogen in is different according to the temperature of expansion through thermal treatment at extremely high speed. From Fig. 2A, it could be seen that NG300 indicates pyridinic-N and pyrrolic-N structures in high proportion, in contrast to graphitic-N in low proportion. As the temperature rises to 600 °C, it can be noticed that pyrrolic-N reduces in proportion and graphitic-N rises in proportion (Fig. 2B). Such doped N atoms would decorate the graphene planar sheet and introduce a change in the Fermi level, engendering the doping effects and opening the band gap of the graphene [35]. At the temperature of 900 °C, the main elements of NG900 are pyridinic-N and graphitic-N (Fig. 2C). Fig. 2D indicates the N1s spectrum of graphene. As what was predicted previously, there were not obvious peaks. The results mentioned above as well as the discussion for the XPS N1s spectra prove the nitrogen atoms succeeded in doping into graphene and transforming into four nitrogen-mixed frameworks in the graphene layers. Under the circumstance of the temperature of expansion through thermal treatment at extremely high speed rising from 300 to 900 °C, the ratios of nitrogen-doped configuration on NGs can be under control.

The electrochemical performance of maltol went through investigation at diverse revised electrodes with the use of cyclic voltammetry (CV) in pH 8.2 boric acid-borax buffer. Fig. 3 indicates cyclic voltammograms filed at bare GCE and NG600 within and without 10 μM maltol at a scan rate of 100 mV/s. Moreover, the result indicates that reactants do not adsorb on the electrode surface. The reaction of maltol on the NG/GCE should be a diffusion-controlled process [36].

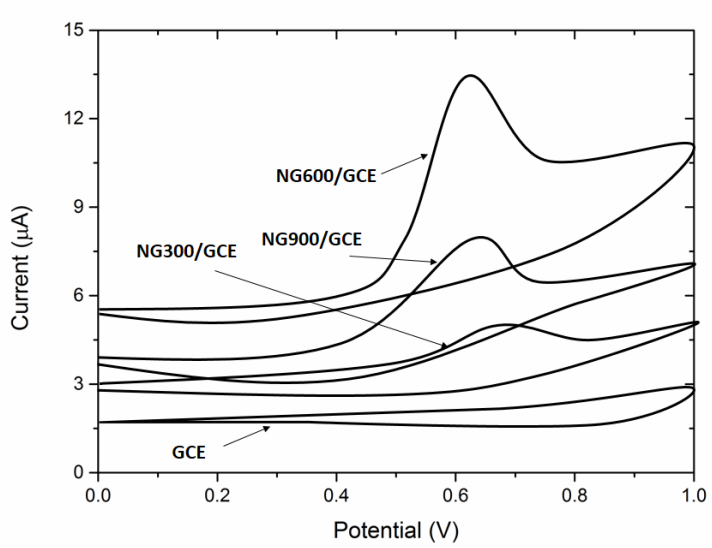

Figure 3. Cyclic voltammograms of bare GCE and NG600 in pH 8.2 boric acid−borax buffer in presence of 10 μM maltol. Scan rate: 100 mV/s.

Curve a shows that a small ultimate point with the oxidation maximum potential at about 0.62 V is obviously noticed on bare GCE, indicating that maltol's oxidation performance is pretty under leveled on the bare GCE appearance. It is interesting that the oxidation peak rises greatly on the appearance of NG600-modified GCE, showing that NG600 that was prepared previously is more active for maltol's oxidation. In contrary to bare GCE, NG600 ternary core-shell material has been confirmed to possess electrode area that is in a larger scale. Meanwhile it has been proved that electron shifts faster. Thus, there is a significant enhancement of oxidation activity for maltol on NG600 appearance. Besides, there is a clear decline in oxidation maximum current of maltol during the second and third anodin c sweeps, which indicates the enhanced adsorbing capacity of oxidation product of maltol on electrode appearance. As a result, the oxidation maximum current in the first anodic sweep is put into record to analyse maltol for the purpose of achieving sensitivity of elevated degree. What is more, researchers also searched into the CV responses of bare GCE and NG600/GCE without the presence of maltol, indicating basically ordinary curves.

How maltol reacts electrochemically was put into further examination with the use of square wave voltammetry (SWV), with corresponding results shown in Fig. 4. In pH 8.2 boric acid-borax buffer and after 60-s accumulation, the oxidation maximum figure that could be hardly noticed occurred on the bare GCE (curve a), indicating gradual electron shift. However, the response is greatly enhanced by 2.4 times at NG300/GCE (curve b). The reason why the maximum current on the appearance of NG300 is elevated is graphene's fantastic electrochemical trait. On the other hand, it is worth mentioning that the oxidation signal of maltol on NG300/GCE and NG600/GCE is smaller than that on the surface of NG600/GCE. This outcome might be due to the annealing effect that the NG600 restored the best electrochemical performance in comparison to others. In addition, the SWV response of NG600 /GCE without the presence of maltol also go through research (curve d), without oxidation wave obviously noticed [37]. To conclude, the comparisons obviously manifest NG sensing platform is potential for electrochemical detection with high sensitivity.

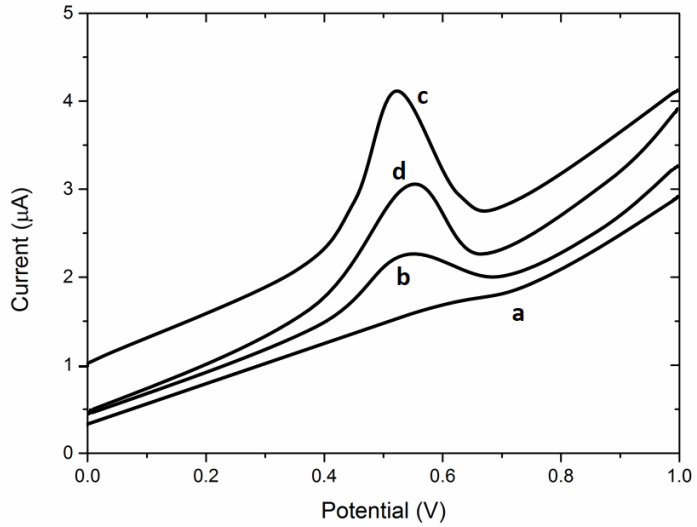

Figure 4. SWV graphs of bare GCE (a), NG300/GCE (b) NG600 (c) and NG900/GCE (d) in pH 8.2 boric acid-borax buffer containing 5.0 μM maltol. Condition: frequency: 15 Hz, scan rate: 40 mV/s, amplitude: 25 mV.

The electrochemical performances of maltol on NG600/GCE with diverse scan rates have been put into examination with the use of CV. The oxidation peak is noticed for maltol, and the oxidation ultimate current (I_p, μA) rises according to the scan rate (v, mV/s). Thus maltol's oxidation could be regarded as an irreversible process controlled by adsorption. For such a reaction, there is a term, Laviron's equation, explaining the relationship between scan rate and peak potential (E_p, V). One electron is engaged in maltol's oxidation, in accordance with the issued outcomes [38, 39]. The oxidation maximum potentials of maltol in boric acid-borax buffer solutions with diverse pH figures went through research for the discussion of shifted protons' number. Such outcomes indicate that E_p shifts negatively with elevating the pH figure, while the slope figure is −60 mV/pH which nearly catches up with the theoretical −59 mV/pH, showing there are evenly shifted electrons and protons in number. On the basis of the outcomes stated above, there could be a conclusion that the maltol's electrochemical oxidation could be regarded as a one-proton and one-electron process. Thus, the redox electrode reaction of maltol was a one-charge-one-proton process, which is agree with the reports in the literature [40, 41].

Diverse pulse voltammetry (DPV) was applied to research how peak currents relates to maltol concentrations, for the purpose of gaining more optimized sensitivity and symmetrical peak morphs. Fig. 5 shows voltammograms with diverse maltol densities. The maximum currents manifested a linear relationship with maltol concentration ranging from 0.05 to 70 μM, as well as with a linear equation of $i_p = 12.514 + 13.87C$ and coefficient of 0.993, in which i_p is the oxidative maximum current in nA and C represents the concentration of maltol in μmol/L. The restricting line of detection through calculation at $S/N = 3$ was 0.03 μM, which is more sensitive than that of other ways, manifesting the merit of this approach to maltol detection. The sensitivity of the proposed sensor was compared with that of other reported modified electrodes and the results were presented in Table 2. For gaining reproducible outcomes, the suggested sensor was then put into exposure to a cycle potential scan of many forms in the potential range between 0.3 and 0.8 V in a blank $NH_3 \cdot H_2O$–NH_4Cl (pH 9.1) buffer solution until the very background CV curve was gained. Through such processing, the experimental repeatability can remain successfully. There is a relevant standard deviation (RSD) of twelve successive scans, namely 1.23%, for 0.5 mM maltol. Under the condition of being dry, in spite of being stored for nearly ten days, no obvious change of the current response was detected, showing that indicating the NG600/GCE is pretty stable. The generation related reproducing capacity of the suggested GCE also went through investigation. The repeatability of six separately generated electrodes indicated a favorable RSD value of 3.7% for detecting the 0.5 mM maltol solution.

Table 2. Comparison of the present NG600/GCE with other maltol determination methods.

Method	Linear detection range	Detection limit	Reference
GCE	10 to 60 μM	5 μM	[41]
HPLC-UV	4.0–76.0 mg/L	1.6 mg/L	[42]
Hanging mercury drop electrode	0.05-3.5μM	—	[43]
NG600/GCE	0.05 to 70 μM	0.03 μM	This work

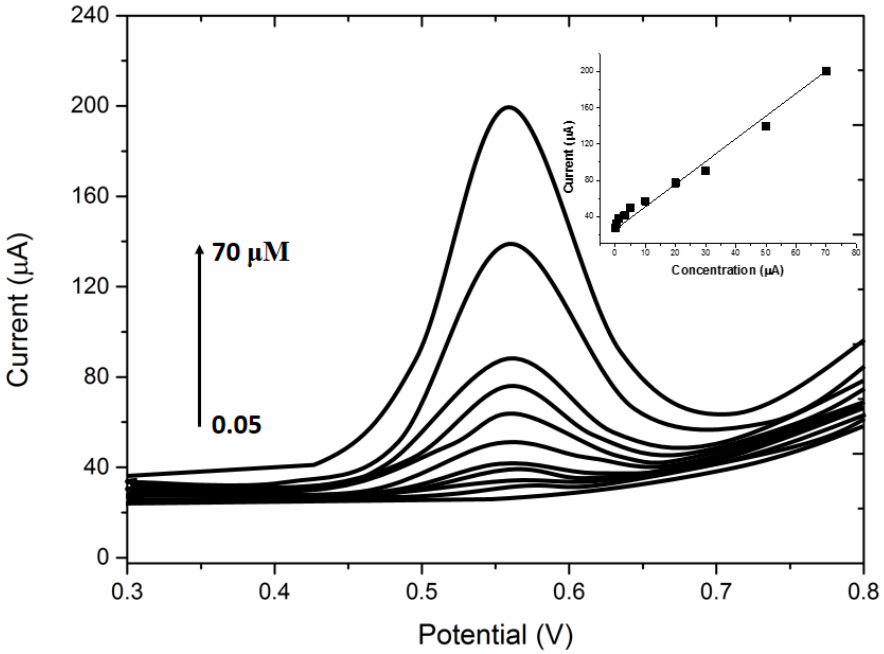

Figure 5. Differential pulse voltammograms with different concentrations of maltol at the NG600/GCE under optimum conditions. Condition: 0.1 M B-R buffer solution (25 °C, scan rate 0.05 V/s)

As to the real analytical application of the approach put forward, the effect of diverse species possible to exist in samples of food and beverage were put into detailed evaluation. Experiments were conducted in a maltol (0.5 mM) solution spiked with diverse excessive quantity of such species under the same experimental conditions. The largest quantity which brought about a relative error of <±5% for maltol determination is regarded to be the ultimate restricting line for exotic species. It was found that 500-fold Ca^{2+}, Na^{+}, Mg^{2+}, CO_3^{2-}, SO_4^{2-}, citrate ion, ascorbic acid, tartaric acid, alcohol, sucrose, and ethyl acetate brought about hardly noticeable interference in the quantitative analysis of maltol with the selected experiment conditions. With the existence of 10-fold uric acid, the anodic maximum figure of maltol maintained pretty stable with nearly no change, while 50-fold uric acid could result in great changes of the background current due to its redox performance as well as adsorption at the electrode.

Table 3. Interference result of determination of maltol with other common species.

Interference species	Current change (%)	Interference species	Current change (%)
Ca^{2+}	3.22	Na^{+}	0.57
Mg^{2+}	-0.54	CO_3^{2-}	-2.88
SO_4^{2-}	-0.73	citrate ion	-3.68
ascorbic acid	2.10	tartaric acid	4.37
alcohol	2.99	sucrose	0.07
ethyl acetate	4.85		

The outcomes indicated that the proposed approach performed well in selectivity for the determination of maltol.

4. CONCLUSION

To conclude, a favourable approach has been proposed for the preparation of nitrogen-doped graphene (NG). The NG was adopted to be a new electrochemical strengthened material for fabricating electrochemical platform for maltol determination in the field of food, which indicated sound linear range (0.05–70 μM) as well as under levelled detection limit (0.02 μM). We hold the belief that the proposed detection method launches a new electrochemical detection mechanism, enable the semiconductor materials to be widely applied, as well as enlightens further fusing of electrochemical technique and analytical approaches.

Reference

1. Y. Lai, W. Pan, D. Zhang and J. Zhan, *Nanoscale*, 3 (2011) 2134.
2. C.V. Borlongan, S. Polgar, T.B. Freeman, R.A. Hauser, D.W. Cahill and P.R. Sanberg, *Neurodegeneration A Journal for Neurodegenerative Disorders Neuroprotection & Neuroregeneration*, 5 (1996) 189.
3. N. Kaneko, H. Yasui, J. Takada, K. Suzuki and H. Sakurai, *Journal of Inorganic Biochemistry*, 98 (2004) 2022.
4. L.R. Bernstein, T. Tanner, C. Godfrey and B. Noll, *Metal-Based Drugs*, 7 (2000) 33.
5. X. Liu, Y. Wang, J. Kong, C. Nie and X. Lin, *Anal Methods*, 4 (2012) 1012.
6. M.A.U. Mehedi, A.H. Molla, P. Khondkar, S. Sultana, M.A. Islam, M.A. Rashid and R. Chowdhury, *Asian Journal of Chemistry*, 22 (2010) 2611.
7. Y. Ni, Y. Wang and S. Kokot, *Food Chemistry*, 109 (2008) 431.
8. M. Skerget, P. Kotnik, M. Hadolin, A.R. Hras, M. Simonic and Z. Knez, *Food Chemistry*, 89 (2005) 191.
9. W.S. Yeung, G.A. Luo, Q.G. Wang and J.P. Ou, *Journal of Chromatography B Analytical Technologies in the Biomedical & Life Sciences*, 797 (2003) 217.
10. Y. Ni, J. Bai and L. Jin, *Anal. Chim. Acta.*, 329 (1996) 65.
11. A. Jiménez-Escrig, I. Jiménez- Jiménez, R. Pulido and F. Saura- Calixto, *Journal of the Science of Food & Agriculture*, 81 (2001) 530.
12. B. Dimitrios, *Trends in Food Science & Technology*, 17 (2006) 505.
13. S. Malovaná, F.J.G.A. Montelongo, J.P. Pérez and M.A. RodríGuez-Delgado, *Anal. Chim. Acta.*, 428 (2001) 245.
14. F. Chekin and M. Yazdaninia, *Russian Journal of Electrochemistry*, 50 (2014) 967.
15. J.B. Wu, Y. Lin, X.H. Xia, J.Y. Xu and Q.Y. Shi, *Electrochimica Acta*, 56 (2011) 7163.
16. B.J. Sanghavi and A.K. Srivastava, *Anal. Chim. Acta.*, 706 (2011) 246.
17. B.J. Sanghavi and A.K. Srivastava, *Electrochimica Acta*, 55 (2010) 8638.
18. H.Y. Ho, W.C. Lin, S. Kitanaka, C.T. Chang and J.B. Wu, *Journal of Food & Drug Analysis*, 16 (2008)
19. Y.H. Fan, S.Y. Bi, Y.Y. Li, C.F. Bi and S.T. Xie, *Russian Journal of Coordination Chemistry*, 34 (2008) 772.
20. J. Chen, M. Gajdardziska-Josifovska, C. Hirschmugl, E. Mattson, H. Pu and M. Weinert, *Carbon Techniques*, 28 (2016) 35.

21. J. Zhao, L. Zhang, T. Chen, H. Yu, L. Zhang, H. Xue and H. Hu, *Electrochimica Acta*, 189 (2016) 175.
22. D. Ji, H. Zhou, J. Zhang, Y. Dan, H. Yang and A. Yuan, *Journal of Materials Chemistry A*, 4 (2016) 8283.
23. Z. Su, H. Wang, K. Tian, F. Xu, W. Huang and X. Tian, *Composites Part A Applied Science & Manufacturing*, 84 (2016) 64.
24. S. Guo, S. Dong and E. Wang, *Acs Nano*, 4 (2010) 547.
25. T. O. Wehling, †, K. S. Novoselov, S. V. Morozov, E. E. Vdovin, M. I. Katsnelson, a. A. K. Geim and A.I. Lichtenstein†, *Nano Letters*, 8 (2007) 173.
26. Y. Wang, Y. Shao, D.W. Matson, J. Li and Y. Lin, *Acs Nano*, 4 (2010) 1790.
27. S.Y. Yang, K.H. Chang, Y.L. Huang, Y.F. Lee, H.W. Tien, S.M. Li, Y.H. Lee, C.H. Liu, C.C.M. Ma and C.C. Hu, *Electrochemistry Communications*, 14 (2012) 39.
28. Z. Wen, X. Wang, S. Mao, Z. Bo, H. Kim, S. Cui, G. Lu, X. Feng and J. Chen, *Adv. Mater.*, 24 (2012) 5610.
29. Y. Wang, Y. Shao, D.W. Matson, J. Li and Y. Lin, *ACS nano*, 4 (2010) 1790.
30. D. Geng, Y. Chen, Y. Chen, Y. Li, R. Li, X. Sun, S. Ye and S. Knights, *Energy & Environmental Science*, 4 (2011) 760.
31. Y.-H. Lee, Y.-F. Lee, K.-H. Chang and C.-C. Hu, *Electrochemistry Communications*, 13 (2011) 50.
32. M. Seredych, D. Hulicova-Jurcakova, G.Q. Lu and T.J. Bandosz, *Carbon*, 46 (2008) 1475.
33. D. Hulicova, M. Kodama and H. Hatori, *Chemistry of materials*, 18 (2006) 2318.
34. Y. Sun, C. Li, Y. Xu, H. Bai, Z. Yao and G. Shi, *Chemical Communications*, 46 (2010) 4740.
35. L. Liu, S. Ryu, M.R. Tomasik, E. Stolyarova, N. Jung, M.S. Hybertsen, M.L. Steigerwald, L.E. Brus and G.W. Flynn, *Nano letters*, 8 (2008) 1965.
36. J. Zhou, K. Zhang, Y. Li, K. Li and B. Ye, *Analytical Methods*, 4 (2012) 3206.
37. T. Gan, J. Sun, M. Yu, K. Wang, Z. Lv and Y. Liu, *Food chemistry*, 214 (2017) 82.
38. M. Chao and X. Ma, *Russian Journal of Electrochemistry*, 50 (2014) 1065.
39. J. Ma, B. Zhang, Y. Wang, X. Hou and L. He, *Journal of Separation Science*, 37 (2014) 920.
40. M.J. Portela, Z.G. de Balugera, M.A. Goicolea and R.J. Barrio, *Anal. Chim. Acta.*, 327 (1996) 65.
41. J. Di, S. Bi and F. Zhang, *Talanta*, 63 (2004) 265.
42. Y. Ni, Y. Wang and S. Kokot, *Food Chemistry*, 109 (2008) 431.
43. M.G.F. SALES, S.A. ALMEIDA and M.C.V. VAZ, *Journal of Food and Drug Analysis*, 16 (2008)